

Reverberation Radii of Dust Holes in Active Galactic Nuclei

V.L. Oknyanskij

*Sternberg State Astronomical Institute, Moscow State University,
 Universitetskij Prospekt 13, Moscow, 119899, Russia*

Keith Horne

*Physics and Astronomy, University of St. Andrews, North Haugh, St.
 Andrews KY16 9SS, Scotland, United Kingdom*

Abstract. It is generally accepted that near-infrared 2 to 5 μm emission from Seyfert galaxies and QSOs is produced by heated dust. The dust (graphite grains) cannot survive inside a critical distance from the nucleus inside which radiation from the central source evaporates dust, leaving a hole in the dust distribution. The radii of these dust holes can be estimated from the time delayed variations seen in near-infrared light curves.

We collect published measurements of time delays between optical (or UV) and near-infrared (*JHKL*) variations in AGNs, reanalyze some of them, and derive several new delay measurements from published photometric data. We thereby infer the radii of the dust-free zones around Seyfert galaxies NGC 4151, 7469, 2992, 4593, 3783, 3786, 1566, 6814, Fairall 9, and the QSO GQ Comae.

We suggest that the dust is generally distributed as a ring or flattened disk with a central hole. Radiation in the *K* band then arises from dust located just outside the radius of the hole. The dust may need to arise from thick clouds to explain rapid recovery of the dust emission after strong outbursts.

For this sample of 10 active galaxies with redshifts $z < 0.165$, we find that the inferred dust-hole radius increases with ultraviolet luminosity as $R \propto L_{\text{UV}}^{1/2}$. Comparison with predictions of simple dust sublimation theory indicates remarkable agreement. This implies that the dust population in AGNs cannot be strongly dependent on the luminosity.

1. Introduction

Circumnuclear dust is thought to be the source of the broad infrared bump seen in the spectral energy distributions of active galactic nuclei (AGNs). The dust (graphite grains) cannot survive at distances from the nucleus closer than a critical radius where the dust reaches its sublimation temperature (for most heat-resistant graphite particles the temperature is 1500–2000 K, see Barvainis 1987). As the luminosity of nucleus increases, an evaporation wave should move

outward, clearing dust from the inner region, and leaving a hole in its previous domain. Dust may then reform or migrate inward in time. The equilibrium radius inside which dust is absent should increase with the nuclear luminosity.

Radii can be estimated using time delays. A small increase in luminosity raises the temperature of the dust outside the sublimation zone, increasing its infrared emission. Light-travel time measures the distance from the nucleus out to the radius where the ultraviolet emission is reprocessed into infrared emission from dust.

Time delays are not entirely trivial to measure because the light curve variations are erratic. Several cross-correlation results on time delays between NIR and optical (or UV) variations have been reported in the literature (Penston et al. 1974; Oknyanskij 1993; Oknyanskij et al. 1999; Oknyanskij 1999; Clavel et al. 1989; Glass 1992, 1998; Nelson 1996; Baribaud et al. 1992).

In Sec. 2 we briefly discuss measurements of optical (UV) to NIR time delays in all cases we have found in the literature. We reanalyze some of the published time delays, and present new time delay results for several objects. This combination of our own results with those made by other authors gives us the opportunity to examine the correlation between time delay and luminosity (Sec. 3). Observational constraints on the geometry of the NIR emission region and dust sublimation theory are briefly sketched and discussed in Sec. 4.

2. Near-Infrared Time Delays in AGNs

Table 1 collects published and new measurements of time delays between variations at near-infrared wavelengths relative to those at optical or ultraviolet wavelengths for our sample of 9 Seyfert galaxies and 1 QSO. We have used the “Modernized Cross-Correlation Function” (MCCF) method to estimate time delays, with corresponding error estimates obtained as described in Oknyanskij (1993) and Oknyanskij et al. (1999). We note that measured time delays between optical and *J* band variations are usually compatible with zero, while at longer wavelengths the *H*, *K*, and *L* bands usually give substantially larger time delays. Taking this into account, we therefore report time delays relative to *J* in several cases where no suitable optical light curves were available. Below we briefly discuss our time delay analysis of each object, deferring details to a future publication.

2.1. NGC 4151

NGC 4151 is the brightest active galactic nucleus (AGN), displaying large amplitude near-infrared (NIR), optical, ultraviolet (UV), soft X-ray, and hard X-ray variability. Rapid NIR variability of NGC 4151 was discovered by Fitch, Pacholczyk, & Weymann (1967) and confirmed by Pacholczyk (1971). The first well-sampled and accurate time series of NIR (*JHKLM*) photoelectric measurements were obtained independently between late 1969 and 1980 by several groups of observers (Penston et al. 1971, 1974; Cutri et al. 1981; O’Dell et al. 1978; Lebofsky & Rieke 1980). After a five-year gap, *JHKL* photoelectric monitoring resumed at the Crimean Station of the SAI (Taranova & Shenavrin 1997; Lyuty et al. 1998; Oknyanskij et al. 1999).

Table 1. Optical–Infrared Time Delays in AGNs

Object	Delay (days)	Bands	$\log L_{UV}$ (erg s^{-1})	Reference
NGC 4151 (Event A)	30 – 60		43.6	Penston 1974 Oknyanskij 1993 this paper
	18 ± 6	$K(U)$		
	26 ± 6	$L(U)$		
NGC 4151 (Event B)	~ 6	$J(UBV)$	44.0	Oknyanskij et al. 1999
	8 ± 4	$H(UBV)$		
	35 ± 8	$K(UBV)$		
	97 ± 10	$L(UBV)$		
Fairall 9	-20 ± 100	$J(UV)$	45.9	Clavel et al. 1989
	250 ± 100	$H(UV)$		
	385 ± 110	$K(UV)$		
	410 ± 100	$L(UV)$		
NGC 3786 (Mrk 744)	32 ± 7	$K(V)$	42.7	Nelson 1996
NGC 3783	80 – 90	$K(U)$	43.9	Glass 1992
NGC 7469	-	$JHKL$	44.2	Glass et al. 1998 Oknyanskij 1999 This work
	40 ± 20	$K(J)$		
	73 ± 15	$L(J)$		
	52 ± 15	$K(U)$		
	60 ± 10	$L(U)$		
GQ Comae	~ 250	$K(UV)$	46.1	Sitko et al. 1993 Oknyanskij 1999
	~ 700	$L(UV)$		
	260 ± 20	$K(V)$		
	750 ± 20	$L(V)$		
NGC 6814	< 15	$K(V)$	—	Nelson 1997, 2000
NGC 1566	30 – 60	$K(H\alpha)$	43.0	Baribaud et al. 1992 This work
	< 20	$K(J)$		
NGC 2992	—	$JHKL$	43.5	Glass et al. 1998 This work
	18 ± 10	$K(J)$		
	84 ± 30	$L(J)$		
NGC 4593	> 8	$K(UV)$	43.9	Santos-Lleó et al. 1994 This work
	7.5 ± 10	$H(J)$		
	20 ± 10	$K(J)$		
	36 ± 15	$L(J)$		

NGC 4151 is often considered a typical Sy 1 or Sy 1.5 type AGN, but is also typical of objects that rapidly change their Seyfert class. NGC 4151 passed through a very deep minimum of activity during 1981–1988. Following Lyuty & Doroshenko (1999), we refer to the 1968–1980 interval, before the minimum, as Event A and to 1989–1999 as Event B. The central source’s mean luminosity during Event A is several times lower than in Event B. In 2000, the object again entered a very low-luminosity state, and may cross another minimum with spectral type close to Sy 1.9. The time delay analysis of the data has been done independently for Events A and B.

The first published report of a preliminary time delay of about 1–2 months between NIR and optical variability in NGC 4151 was obtained by visual inspection of the light curves (Penston et al. 1971, 1974). A cross-correlation analysis of the K light curve during Event A and the U light curve (Lyuty 1972, 1977) revealed K variations lagging behind those in U by 18 ± 6 d (Oknyanskij 1993).

Here we report results of a cross-correlation analysis of the L band variations of NGC 4151 during Event A. We assembled an L light curve from several independent datasets (Cutri et al. 1981; O’Dell et al. 1978; Lebofsky & Rieke 1980; Bassani et al. 1986; McAlary et al. 1983). The resulting L light curve, with 28 points remaining after removing observations with errors larger than 10%, has significantly fewer points than the K light curve used previously. We made aperture corrections, reducing the data to a common $17''$ aperture, based on observations with a range of aperture sizes (McAlary et al. 1983). The L data of Penston et al. (1971, 1974) were omitted in view of their large errors. After converting the L and U light curves from magnitudes to fluxes, our MCCF analysis reveals that L variations lag behind U variations by 26 ± 6 d. This is larger than the 18 ± 6 d delay found at K , as expected for dust temperature falling with radius, but one may worry that the data and time interval are not exactly the same. Selecting K data from Cutri et al. (1981) only (the most significant dataset in the L light curve), we find K lagging U by 15 d. While this difference in the L and K delays for NGC 4151 in Event A is not statistically very significant, similar differences (time delay increasing with NIR wavelength) are found for several objects (see Table 1).

2.2. Fairall 9

Table 1 reports time delays for Fairall 9 for NIR $JHKL$ variations relative to UV variations as found by Clavel et al. (1989). The delay increases with wavelength from -20 ± 100 d at J , consistent with zero, up to 410 ± 100 d at L . Although these Fairall 9 delays are most often cited in publications, they are based on less representative datasets than for NGC 4151 and several of the other objects discussed below.

2.3. NGC 3783

Glass (1992) reports a time delay of 80–90 d between U and K variations in NGC 3783. This is one of the best determined results on time lags between optical and NIR variability in AGNs.

2.4. NGC 3786

For NGC 3786 (Mrk 744), a cross-correlation delay of 32 ± 7 d with K variations lagging V variations is reported by Nelson (1996). We note that light curve is rather sparsely sampled so that the delay refers mainly to a single large event in the two light curves.

2.5. NGC 7469

NGC 7469 is one of the most intensively investigated Seyfert galaxies. Glass et al. (1998) discuss long-term NIR monitoring, using for comparison UBV light curves from observations made in the Crimea (see references in the paper). A cross-correlation analysis was not attempted. Glass et al. expected a time delay of about 130 d at K , based on the dust sublimation theory (Barvanis 1987), but there was insufficient overlap between the optical and NIR datasets to test this prediction. Using J in lieu of an optical light curve, Oknyanskij (1999) finds delays of 40 ± 20 d at K and 73 ± 15 d at L , significantly less than the predicted value. These small delays are confirmed here by a new analysis using optical photometry obtained in the Crimea (Doroshenko, Lyuty, & Rakhimov 1989; Lyuty 1999) supplemented with datasets obtained by Rakhimov (1989). Our MCCF analysis of the resulting U light curve with 161 nightly mean data points and HKL data from Glass et al. gives time delays of 52 ± 15 d at K and 60 ± 10 d at L , as presented in Table 1.

2.6. GQ Com

GQ Comae (PG 1202+281, $z = 0.165$) is one of the most strongly and rapidly varying radio-quiet QSOs. Sitko et al. (1993) discuss optical, UV, and NIR photometry spanning about 3 years. Delays of about 250 d at K and 700 d at L are found relative to UV variations based on a discrete cross-correlation function (DCF) analysis (Edelson & Krolik 1988) as well as visual inspection of the light curves. As the DCF analysis may be affected by the rather small number of points (only 17 UV measurements), Oknyanskij (1999) re-analyzed the K and L light curves relative to the V light curve (36 points), finding delays of 260 ± 20 d at K and 750 ± 20 d at L .

2.7. NGC 6814

Nelson (1997) reports that NGC 6814 showed a lag time between V and K variations consistent with zero. From a subsequent private communication (Nelson 2000), we can report that the time delay is less than 15 d. As NGC 6814 is a low luminosity Seyfert galaxy, a small time delay, possibly as little as a few days, may be expected. An intense monitoring program with daily cadence would be needed to have a chance to find so small a delay.

2.8. NGC 1566

Baribaud et al. (1992) find a delay of 7 weeks between UV and K variations in NGC 1566, a result often cited in the literature. Our analysis of data published in the paper shows that the time delay between J and K variations is consistent with zero and in any case less than 20 d. Baribaud et al. used an $H\alpha$ light curve, suspecting that it may relate directly to the UV photon light curve. However,

the accuracy of the $H\alpha$ measurements, 10% or worse, is worse than the accuracy of the NIR photometry. In view of the limited time sampling, Baribaud et al. did not attempt a cross-correlation analysis, but rather estimated delays by inspecting several events in the light curves. In our opinion this result has low statistical significance, and we therefore prefer the smaller delay we find from the J vs. K cross-correlation analysis.

2.9. NGC 2992

The long-term $JHKL$ light curves of NGC 2992 obtained by Glass (1998) feature an apparent outburst in 1988 with a roughly exponential decay. The event amplitude is largest at L and smallest at J . Glass did not attempt to investigate time delays as available for this were only 6 $UBVRI$ points with variations less than 0.1 mag in the interval JD 2446827 – 2447681 (Winkler et al. 1998). By using J data in place of an optical light curve, our MCCF analysis yields delays of 18 ± 10 d between J and K variations, and 84 ± 30 d between J and L .

2.10. NGC 4593

$JHKL$ photometry of NGC 4593 are discussed by Santos-Lleó et al. (1994). There are only 22 observation dates for JHK , and 20 for L . The paper uses UV observations to conclude that the time delay at K relative to the UV variations is at least 8 d. Using photometric data from the paper, our MCCF analysis yields time delays of 7.5 ± 10 d at H , 20 ± 10 d at K , and 36 ± 15 d at L , relative to J variations.

3. Dependence of Time Delay on Luminosity

Using the delay measurements collected in Table 1, we now examine the dependence of near-infrared time delays on the UV luminosity (L_{UV}) in order to compare the result with theoretical predictions.

It should be noted that obtaining reliable estimates of L_{UV} that allow for host-galaxy contamination, all types of possible obscuration, and time variability of the objects is no easy task. Some of the objects have never been observed at UV or X-ray wavelengths. Even in good cases with observations of the 1100–3000 Å spectrum, the spectral range 150–1150 Å is not observable. For Fairall 9, Clavel et al. (1989) give a 50% uncertainty for L_{UV} .

We suggest that for each of the objects in Table 1 the uncertainty in L_{UV} cannot be smaller than 50%. The estimates of L_{UV} for the same object are often different in different publications, reflecting different methods of estimation, different spectral regions considered, and whether or not factors like variability are taken into consideration.

To minimize the possibility of subjective bias in choosing the values of L_{UV} , for this paper we simply adopt the L_{UV} values quoted in the publications reporting the NIR time delays or NIR data that we used for our time delay analysis. Fortunately, we can do this for all objects except NGC 6814. We have corrected the L_{UV} values in Table 1 to a common value of $H_0 = 50 \text{ km s}^{-1} \text{ Mpc}^{-1}$.

Figure 1 plots the observed K band time delays against the adopted luminosity, showing a significant correlation (the correlation coefficient is 0.87).

The slope of a best-fit regression line (not shown) is 0.515, consistent with the “expected” value 0.5.

3.1. Luminosity and Redshift Corrections

It would be best to correct the luminosity estimates as far as possible to a common system, but we defer this to future work while limiting the present discussion to two obvious examples. Two points on Fig. 1, corresponding to NGC 3786 and NGC 3783, fall well to the left of the other points. For NGC 3786, Nelson (1996) used a theoretical model to estimate $L_{UV} \approx 10^{42.7}$ erg s⁻¹, since no X-ray or UV observations were available. We may alternatively estimate L_{UV} by assuming that the spectral energy distribution of NGC 3786 is similar to that of NGC 4151. Comparing NIR fluxes observed in high states of both objects then suggests $L_{UV} \approx 10^{44}$ erg s⁻¹. Applying the same method to NGC 3783 yields $L_{UV} \approx 10^{44.6}$ erg s⁻¹ in place of $10^{43.9}$ erg s⁻¹ from Glass (1992). Glass noted that his estimate for NGC 3783 may be somewhat low if one corrects for the power emitted by the dust. These two corrections, indicated in Fig. 1 by arrows pointing to the corrected values (open circles) clearly improve the correlation.

The observed time delays discussed above and reported in Table 1 also require a correction for the redshift. This correction is largest for GQ Com at $z = 0.165$. The observed time delay τ_o and effective wavelength λ_o are both larger by a factor $1 + z$ compared with their values τ_e and λ_e in the emission rest frame. Taking GQ Com as an example, the observed delay $\tau_o = 260$ d for the K band at $\lambda_o = 2.2$ μm corresponds to a delay $\tau_e = \tau_o/(1 + z) = 223$ d at $\lambda_e = \lambda_o/(1 + z) = 1.9$ μm in the rest frame of GQ Com.

Note in Table 1 that the observed delays increase sharply with wavelength, consistent with the dust temperature decreasing with radius. From theory, the equilibrium dust temperature is $T \propto R^{-B}$ with $B \approx 2.8$ (Barvanis 1987). Since $\tau \approx R/c$ and dust at temperature T emits at wavelength $\lambda \sim hc/4kT$, we expect $\tau \propto \lambda^B$, and hence $\tau_e(\lambda_o) = \tau_o(\lambda_o)(1 + z)^{B-1}$. Adopting $B = 2.8$, the observed K band delay of 260 d corresponds to a K band delay of 340 d in the rest frame of GQ Com. The box on Fig. 1 indicates the redshift-corrected delay for GQ Com. Smaller corrections apply to the other objects.

4. Discussion

The near-infrared emission of active galaxies is widely attributed to circumnuclear dust heated by radiation from the active nucleus. Evidence favoring this interpretation is a change in slope of the spectral energy distribution of active galaxies between the optical and near-infrared spectral regions (Rees et al. 1969). This “1 μm kink” occurs at a wavelength that is independent of the luminosity and corresponds to a temperature $T \approx 1500$ K similar to dust sublimation temperatures.

For a smooth spherically symmetric dust distribution, Barvanis (1987) gives the “evaporation radius” as

$$R_{\text{evap}} = 1.3 L_{46}^{0.5} \left(\frac{T}{1500\text{K}} \right)^{-2.8} \text{ pc}, \quad (1)$$

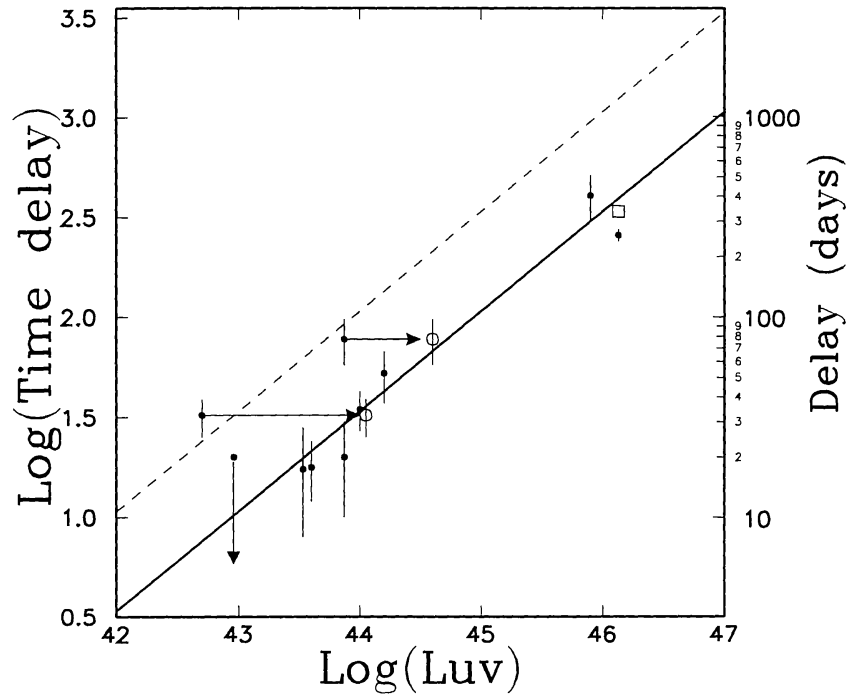


Figure 1. Relationship between infrared time delay and UV luminosity. Points with error bars give time delay measurements (K band) and published values of L_{UV} (corrected to $H_0 = 50 \text{ km s}^{-1} \text{ Mpc}^{-1}$) from Table 1. A box indicates the time delay for GQ Comae after correcting for its redshift. Arrows pointing to open circles indicate suggested corrections to the estimated luminosities of NGC 3783 and NGC 3786. The observations are compatible with the $R \propto L^{1/2}$ relationship predicted by dust evaporation theory. The evaporation limit for exposed dust grains (dashed line; Barvanis 1987) is well above the observations. Dust hiding in clouds can approach closer to the nucleus (solid line; Barvanis 1992, Sitko et al. 1993), giving better agreement with the data.

where T is the grain evaporation temperature, and L_{46} is the ultraviolet luminosity in units of 10^{46} erg s $^{-1}$. Although this relationship is often used in publications, it predicts time delays (dashed line in Fig.1) that are several times larger than those observed.

Spherically symmetric dust regions also contradict HST imaging studies revealing ring or disk-like dust distributions for some objects. If dust regions have similar structures in most AGNs, then we must reject spherically symmetric dust models.

Oknyanskij et al. (1999), using numerical simulations of the time delay distribution, concluded from the narrow range of the observed time delay distribution that the NIR emission region in NGC 4151 cannot be spherically symmetric but may have the shape of a thin ring or torus viewed roughly face-on. Glass (1992) reached a similar conclusion for NGC 3783.

Smooth dust distributions also fail to explain observations of prompt recovery in the near-infrared emission, indicating rapid reformation of dust grains, following luminosity peaks. Barvanis (1992) considered “reformation” and “survival” models with dust grains emerging from dense clouds. This model can be reconciled with observations by introducing an axi-symmetric distribution of clouds concentrated toward the equatorial plane (e.g., Rowan-Robinson 1995). This type of model yields

$$R_{\text{evap}} = 1.1 L_{46}^{0.5} e^{-\tau_{\text{UV}}/2} \left(\frac{T}{1500 \text{ K}} \right)^{-2.8} \left(\frac{a}{0.05 \mu\text{m}} \right)^{-0.5} \text{ pc}, \quad (2)$$

where a is the mean size of the graphite grains, and τ_{UV} is the UV optical depth of the dust clouds. Thus larger grains, and grains shielded from the UV radiation, can approach the nucleus more closely before evaporating. Following Sitko et al. (1993), we adopt $T = 1700$ K, $a = 0.15 \mu\text{m}$, and $\tau_{\text{UV}} = 1$. The result (solid line in Fig. 1) is then in good agreement with the observations.

5. Summary

We have used optical and infrared light curves to estimate infrared time delays in a sample of 10 nearby active galactic nuclei. We interpret the time delays as light travel time from the nucleus out to the inner edge of the dust zone.

Combining our results with time delays for other objects from the literature, we find that dust ring radii increase with luminosity as $R \propto L^{1/2}$. This is consistent with a very simple dust sublimation theory. Although the theoretical sublimation radius is sensitive to the dust composition, the observations suggest a fixed size for dust grains, or at least that the population of dust grains depends only weakly on the luminosity of the object.

Acknowledgements

We thank the Royal Society and PPARC for financial support of this research.

References

Baribaud, T, Alloin, D., Glass, I., & Pelat, D. 1992, A&A, 256, 375

- Barvainis, R. 1987, *ApJ*, 320, 537
Barvainis, R. 1992, *ApJ*, 400, 502
Bassani, R.C., et al. 1986, *ApJ*, 311, 623
Clavel, J., Wamsteker, W., & Glass, I.S. 1989, *ApJ*, 337, 236
Cutri, R.M., et al. 1981, *ApJ*, 245, 81
Doroshenko, V.T., Lyuty, V.M., & Rakhimov, V.Yu. 1989, *Astronomy Letters*, 15, 207
Edelson, R.A., & Krolik, J.H. 1988, *ApJ*, 333, 646
Fitch, W.S., Pacholczyk, A.C., & Weymann, R.J. 1967, *ApJ*, 150, L67
Glass, I.S. 1992, *MNRAS*, 256, 23P
Glass, I.S. 1998, *MNRAS*, 297, 18
Lebedofsky, M.J. & Rieke, G.H. 1980, *Nature*, 284, 410
Lyuty, V.M. 1972, *Astron. Zh.*, 49, 930
Lyuty, V.M. 1977, *Astron. Zh.*, 54, 1153
Lyuty, V.M. 1999, (private communication)
Lyuty, V.M. & Doroshenko, V.T. 1999, *Astron. Zh.*, 25, 403
Lyuty, V.M., Taranova, O.G., & Shenavrin V.I., 1998, *Pis'ma Astron. Zh.*, 24, 243
McAlary, W., McLaren, R.A., McGonegal, R.J., & Maza, Z. 1983, *ApJS*, 52, 341
Nelson, B.O. 1996, *ApJ*, 465, 87
Nelson, B.O. 1997, *PASP*, 109, 342
Nelson, B.O. 2000, private communication
Oknyanskij, V.L., 1993, *Astronomy Letters*, 19, 416
Oknyanskij, V.L. 1999, *Odessa Astronomical Publications*, 12, 99
Oknyanskij, V.L., Lyuty, V.M., Taranova, O.G., & Shenavrin V.I. 1999, *Astronomy Letters*, 25, 483
O'Dell, S.L., Pushchell, J.J., Stein, W.A., & Warner, J.W. 1978, *ApJS*, 38, 267
Pacholczyk, A.G. 1971, *ApJ*, 163, 449
Penston, M.V., et al. 1971, *MNRAS*, 153, 29
Penston, M.V., et al. 1974, *MNRAS*, 169, 357
Rakhimov, V.Yu. 1989, *Bulletin of Astrophys. Inst. (Dushanbe)*, 78, 50
Rees, M.J., Silk, J.I., Werner, M.W., & Wickramasinghe, N.C. 1969, *Nature*, 223, 788
Rowan-Robinson, M. 1995, *MNRAS*, 272, 737
Santos-Lleó, M., et al. 1994, *MNRAS*, 270, 580
Sitko, M.L., Sitko, A.K., Siemiginowska, A., & Szczerba, R. 1993, *ApJ*, 409, 139
Taranova, O.G. & Shenavrin, V.I. 1997, *Astronomy Letters*, 6, 709
Winkler, H., et al. 1998, *MNRAS*, 257, 659